Analysis and Improvement of Image Quality in De-Blocked Images

U. SRINIVAS
M.Tech Student Scholar, DECS,
Dept of Electronics and Communication Engineering,
Nalanda Institute of Engineering and technology,
Sattenapalli (M); Guntur (Dt); A.P, India.

K. SYAM PRASAD
M.Tech, Asst Professor
Dept of Electronics and Communication Engineering,
Nalanda Institute of Engineering and technology,
Sattenapalli (M); Guntur (Dt); A.P, India.

Abstract: *Image quality is a characteristic of an image that measures the perceived image degradation (typically, compared to an ideal or perfect image). Imaging systems may introduce some amounts of distortion or artifacts in the signal, so the quality assessment is an important problem JPEG compression is the most prevalent technique or method for image codec's. But it suffers from blocking artifacts. In this paper a comparison of the perceptual quality of de-blocked images based on various quality assessments metric is done. We study the efficiency of de-blocking algorithms for improving visual signals degraded by blocking artifacts from compression. Rather than using only the perceptually questionable PSNR, we instead propose a block-sensitive index, named PSNR-B, that produces objective judgments that accord with observations. The PSNR-B modifies PSNR by including a blocking effect factor. We also use the perceptually significant SSIM index, which produces results largely in agreement with PSNR-B. Simulation results show that the PSNR-B results in better performance for quality assessment of deblocked images than PSNR and a well-known blockiness-specific index.*

Keywords: *Blocking effect, deblocking, distortion, image quality assessment, quantization.*

I. INTRODUCTION

Many practical and commercial systems use digital image compression when it is required to transmit or store the image over limited resources. JPEG compression is the most popular image compression standard among all the members of lossy compression standards family. JPEG image coding is based on block based discrete cosine transform. BDCT coding has been successfully used in image and video compression applications due to its energy compacting property and relative ease of implementation. After segmenting an image in to blocks of size N×N, the blocks are independently DCT transformed, quantized, coded and transmitted. One of the most noticeable degradation of the block transform coding is the "blocking artifact". These artifacts appear as a regular pattern of visible block boundaries. This degradation is the result of course quantization of the coefficients and of the independent processing of the blocks which does not take in to account the existing correlations among adjacent block pixels [1]. In order to achieve high compression rates using BTC with visually acceptable results, a procedure known as deblocking is done in order to eliminate blocking artifacts.

Blocking effects are common in block-based image and video compression systems. Blocking artifacts are more serious at low bit rates, where network bandwidths are limited. Significant research has been done on blocking artifact reduction [2]–[4]. Most blocking artifact reduction methods assume that the distorted image contains noticeable amount of blocking. The degree of blocking depends upon several parameters, the most important of which is the quantization step for lossy compression. Little research has done on comparing the perceptual quality of de-blocked images. The recent advent of powerful modern image quality assessment (IQA) algorithms[5] that compare well with human subjectively makes this plausible. Here we investigate quality assessment of de-blocked images, and in particular we study the effects of the quantization step of the measured quality of de-blocked images. A de-blocking filter can improve image quality in some aspects, but can reduce image quality in other regards.

We perform simulations on the quality assessment of De-blocked images. We first perform simulations using the conventional peak signal-to-noise ratio (PSNR) quality metric and a state of the art quality index, the structural similarity (SSIM) index. The PSNR does not capture subjective quality well when blocking artifacts are present. The SSIM metric is slightly more complex than the PSNR, but correlates highly with human subjectively. We also propose a new de-blocking quality index that is sensitive to blocking artifacts in de-blocked images. We name this peak signal-to-noise ratio including blocking effects (PSNR-B). The simulation results show that the proposed PSNR-B correlates well with subjective quality and with the SSIM index, and performs much better than the PSNR.

We study a variety of image and video de-blocking algorithms, including low pass filtering, projection onto convex sets (POCS), and the H.264 in-loop filter. The image improvements afforded by these algorithms is measured using the PSNR, PSNR-B, and SSIM. Rather than relying on PSNR, which correlates poorly with subjective judgment, we utilize PSNR-B which is designed specifically to assess blocky and de-blocked images (but has no proven perceptual significance) in conjunction with the SSIM index, which is perceptually significant, but has not been demonstrated on de-blocked images[6]

To remove blocking effect, several de-blocking techniques have been proposed in the literature as post process mechanisms after JPEG compression, depending on the angle from which the blocking problem is tackled. If de-blocking is viewed as an estimation problem, the simplest solution is probably just to low pass the blocky JPEG compressed image. More sophisticated methods involve iterative methods such as projection on convex sets and constrained least squares[7],[8]

II. BASED ON QUALITY ASSESSMENT

We consider the class of quality assessment (QA) methods that are full-reference (FR) QA, which compares the test (distorted) image with a reference (original) image. In this paper, the distorted images will ostensibly suffer from blocking artifacts or from the residual artifacts following de-blocking.

A. *Peak Signal To Noise Ratio(PSNR):*

The simplest and most widely used FR QA metrics are the peak signal-to-noise ratio (PSNR) and the mean-squared error(MSE) [2], [4]. Let and represent the vectors of reference and test image signals, respectively. Let be the vector of error signal between and . If the number of pixels in an image is N, then

$$\mathrm{MSE}(\mathbf{x},\mathbf{y}) = \frac{1}{N}\sum_{i=1}^{N} e_i^2 = \frac{1}{N}\sum_{i=1}^{N}(x_i - y_i)^2 \tag{1}$$

$$\mathrm{PSNR}(\mathbf{x},\mathbf{y}) = 10\log_{10}\frac{255^2}{\mathrm{MSE}(\mathbf{x},\mathbf{y})}. \tag{2}$$

The PSNR is an attractive QA metric since it is mathematically simple and has clear physical meaning. However, the PSNR does not correlate well with perceived visual quality [3]–[6].

B. *Structural Similarity Index Metric(SSIM):*

The structural similarity (SSIM) metric aims to measure quality by capturing the similarity of images [1]. A product of three aspects of similarity are measured: luminance, contrast, and structure. The luminance comparison function **l(x,y)** for reference image **x** and test image **y** is defined as

$$l(\mathbf{x},\mathbf{y}) = \frac{2\mu_x\mu_y + C_1}{\mu_x^2 + \mu_y^2 + C_1} \tag{3}$$

Where □ □□and □ □□are the standard deviation of and, respectively, and C1 is a stabilizing constant.

The structure comparison function is **c(x,y)** defined as

$$c(\mathbf{x},\mathbf{y}) = \frac{2\sigma_x\sigma_y + C_2}{\sigma_x^2 + \sigma_y^2 + C_2} \tag{4}$$

Where □ □□and □ □ are the standard deviation of and , respectively, and C2 is a stabilizing constant.

The structure comparison function **s(x,y)** is defined as

$$s(\mathbf{x},\mathbf{y}) = \frac{\sigma_{xy} + C_3}{\sigma_x\sigma_y + C_3} \tag{5}$$

Where □□□ □ is the correlation between **x** and **y** **C3** is also a constant that provides stability

The SSIM index is obtained by combining the three comparison functions

$$\mathrm{SSIM}(\mathbf{x},\mathbf{y}) = [l(\mathbf{x},\mathbf{y})]^{\alpha}\cdot[c(\mathbf{x},\mathbf{y})]^{\beta}\cdot[s(\mathbf{x},\mathbf{y})]^{\gamma}. \tag{6}$$

The parameters are set as

$$\alpha = \beta = \gamma = 1 \text{ and } C_3 = C_2/2$$

$$\mathrm{SSIM}(\mathbf{x},\mathbf{y}) = \frac{(2\mu_x\mu_y + C_1)(2\sigma_{xy} + C_2)}{(\mu_x^2+\mu_y^2 + C_1)(\sigma_x^2+\sigma_y^2 + C_2)}. \tag{7}$$

Local SSIM statistics are estimated using a symmetric Gaussian weighting function. The mean SSIM index pools the spatial SSIM values to evaluate the overall image quality

$$\mathrm{SSIM}(\mathbf{x},\mathbf{y}) = \frac{1}{M}\sum_{j=1}^{M}\mathrm{SSIM}(\mathbf{x}_j,\mathbf{y}_j) \tag{8}$$

where **M** is the number of local windows over the image, and **Xj** and **Yj** are image patches covered by the **j**'th window

III. QUANTIZATION STEP SIZE AND IMAGE QUALITY

Quantization is a key element of lossy compression, but information is lost. There is a tradeoff between compression ratio and reconstructed image/video quality. The amount of compression and the quality can be controlled by the quantization step. As the quantization step is increased, the compression ratio becomes larger, and the quality generally worsens. However, there has not been a study made of how perceptual quality suffers as a function of step size, or the degree to which de-blocking augments perceptual quality. The emergence of new and powerful IQA indices suggests this possibility.

In block transform coding, the input image is divided into **Lx L** blocks, and each block is transformed independently into transform coefficients. An input image block is transformed into a DCT coefficient block

Figure 1: Block diagram for reference, decoded, and de-blocked images

$$B = TbT^t \tag{9}$$

Where T is the transform matrix and T^t is the transpose matrix of . The transform coefficients are quantized using a scalar quantizer.

$$\tilde{B} = Q(B) = Q(TbT^t) \tag{10}$$

The quantization operator in (10) is nonlinear, and is a many-to-one mapping from R^{L^2} to R^{L^2}

In the decoder, only quantized transform coefficients $\tilde{B}$ are available. The output of the decoder is

$$\tilde{b} = T^t\tilde{B}T = T^tQ(TbT^t)T \tag{11}$$

Let Δ represent the quantization step. It is well known that the PSNR is a monotonically decreasing function of Δ. The SSIM index captures the similarity of reference and test images. As the quantization step size becomes larger, the structural differences between reference and test image will generally increase, and in particular the structure terms**(x, y)** in (5) will become smaller. Hence, the SSIM index would be a monotonically decreasing function of the quantization step size Δ.

IV. DEBLOCKING FILTER AND DISTORTION CHANGE

As before, **x** is the reference (original) image and **y** is the decoded image that has been distorted by quantization errors. Let $\tilde{y}$ represent the de-blocked image and **f** represent the de-blocking operation $\tilde{y} = f(y)$ Fig. 1 shows a block diagram depicting the flow of reference, decoded, and de-blocked images. Let **M(x,y)** be the quality metric between and . The goal of the de- blocking operation **f** is to maximize **M(x,f(y))** given image **y** .

De-blocking is a local operation. The de-blocking operation may improve the appearance of the image in some regions, while degrading the quality elsewhere.
Let be the distortion between the **i**'th pixels of **x** and **y** , expressed as squared Euclidean distance

$$d(x_i, y_i) = \|x_i - y_i\|^2 \tag{12}$$

Next, we define the distortion decrease region (DDR) **A** to be composed of those pixels where the distortion is decreased by the de-blocking operation

$$i \in \mathcal{A}, \text{ if } d(x_i, \tilde{y}_i) < d(x_i, y_i) \tag{13}$$

The amount of distortion decrease for the th pixel in the DDR **A** is

$$\alpha_i = d(x_i, y_i) - d(x_i, \tilde{y}_i) \tag{14}$$

The distortion may also increase at other pixels by application of the de-blocking filter. We similarly define the distortion increase region (DIR) $\mathcal{B}$

$$i \in \mathcal{B}, \text{ if } d(x_i, y_i) < d(x_i, \tilde{y}_i) \tag{15}$$

The amount of distortion increase for the **i**'th pixel β_i in the DIR $\mathcal{B}$ is

$$\beta_i = d(x_i, \tilde{y}_i) - d(x_i, y_i) \tag{16}$$

We define the mean distortion decrease (MDD)

$$\bar{\alpha} = \frac{1}{N} \sum_{i \in \mathcal{A}} (d(x_i, y_i) - d(x_i, \tilde{y}_i)) \tag{17}$$

Where **N** is the number of pixels in the image. Similarly the mean distortion increase (MDI) is

$$\bar{\beta} = \frac{1}{N} \sum_{i \in \mathcal{B}} (d(x_i, \tilde{y}_i) - d(x_i, y_i)) \tag{18}$$

A reasonable approach for designing a de-blocking filter would be to seek to maximize the MDD and minimize the MDI . This is generally a very difficult task and of course, may not result in optimized improvement in perceptual quality. Lastly, let be the mean distortion change (MDC), defined as the difference between MDD and MDI.

$$\bar{\gamma} = \bar{\alpha} - \bar{\beta} \tag{19}$$

If $\bar{\gamma} < 0$, then the de-blocking operation is likely unsuccessful since the mean distortion increase is larger than the mean distortion decrease. We would expect a successful de-blocking operation to yield $\bar{\gamma} > 0$.Nevertheless, these conditions are not equated with levels of perceptual improvement or loss. De-blocking can be considered as an image restoration problem. Let represent the de-blocking operation function and $\mathcal{N}(x_i)$ represent a neighborhood of pixel x_i.

A low pass filter is a simple de-blocking filter. An **L x L** low pass filter can be represented as

$$g(\mathcal{N}(x_i)) = \sum_{k=1}^{L^2} h_k \cdot x_{i,k} \tag{20}$$

While low pass filtering does reduce blocking artifacts, critical high frequency information is also lost and the image is blurred. While the distortion will certainly decrease for some pixels that define the DDR , the distortion will likely increase for a significant number of pixels in DIR . Indeed, it is quite possible that $\bar{\gamma} < 0$ could result. Moreover, blur is perceptually annoying.

A variety of nonlinear methods have been proposed to reduce the blocking artifacts, while minimizing the loss of original information [7]–[14]. For example, de-blocking algorithms based upon projection onto convex sets (POCS) have demonstrated good performance for reducing blocking artifacts and have proved popular [7]–[12]. In POCS, a low pass filtering operation is performed in the spatial domain, while a projection operation is performed in the DCT domain. Typically, the projection operation is a clipping operation on the filtered coefficients, confining these to fall within a certain range defined by the quantization step size. Since the low pass filtering and the projection operations are performed in different domains, forward DCT and inverse DCT (IDCT) operations are required. The low pass filtering, DCT, projection, IDCT operations compose one iteration, and multiple iterations are required to achieve convergence. It is argued that under certain conditions, POCS filtered images converge to an image that does not exhibit blocking artifacts [7], [10], [11]. As another example, the H.264 in-loop de-blocking filter is a key component in the H.264 video coding standard [17]. It is claimed that the in-loop filtering significantly improves both subjective and objective video quality [15]. The key idea of the H.264 in-loop filter is to adaptively select the filtering operation and the neighborhood using the relative pixel location with respect to the block boundary and the local gray level gradient information. Generally, the MDI value is reduced while the MDD value is similar to low pass filtering. The H.264 in-loop filter uses separate 1-D operations and integer multiplications to reduce complexity. However, it still requires a large amount of computation. In fact, the H.264 in-loop filter requires about one-third of the computational complexity of the decoder [15].

V. PSNR INCLUDING BLOCKING EFFECTS

In the following, we propose a new block-sensitive image quality metric which we term peak signal-to-noise ratio including blocking effects (PSNR-B). As the quantization step size increases, blocking artifacts generally become more conspicuous. Blocking artifacts are gray level discontinuities at block boundaries, which are ordinarily oriented horizontally and vertically. They arise from poor representation of the block luminance levels near the block boundaries [18].

The following definitions are relative to an assumed block-based compression tiling, e.g., 8 x 8 blocks as in JPEG compression. For simplicity, assume that an integer number of blocks comprise the image, viz., that horizontal and vertical dimensions are divisible by the block dimension. The definitions apply whether the image is compressed, not-compressed, or de-blocked following decompression.

y_1	y_2	y_3	y_4	y_5	y_6	y_7	y_8
y_9	y_{10}	y_{11}	y_{12}	y_{13}	y_{14}	y_{15}	y_{16}
y_{17}	y_{18}	y_{19}	y_{20}	y_{21}	y_{22}	y_{23}	y_{24}
y_{25}	y_{26}	y_{27}	y_{28}	y_{29}	y_{30}	y_{31}	y_{32}
y_{33}	y_{34}	y_{35}	y_{36}	y_{37}	y_{38}	y_{39}	y_{40}
y_{41}	y_{42}	y_{43}	y_{44}	y_{45}	y_{46}	y_{47}	y_{48}
y_{49}	y_{50}	y_{51}	y_{52}	y_{53}	y_{54}	y_{55}	y_{56}
y_{57}	y_{58}	y_{59}	y_{60}	y_{61}	y_{62}	y_{63}	y_{64}

Figure 2: Example for illustration of pixel blocks

Let $N_{H_B}, N_{H_B^C}, N_{V_B}$ be the number of pixel pairs In $\mathcal{H}_B, \mathcal{H}_B^C, \mathcal{V}_B$ respectively. If B is the block size, then

$$\begin{aligned} N_{H_B} &= N_V \left(\frac{N_H}{B}\right) - 1 \\ N_{H_B^C} &= N_V(N_H - 1) - N_{H_B} \\ N_{V_B} &= N_H \left(\frac{N_V}{B}\right) - 1 \\ N_{V_B^C} &= N_H(N_V - 1) - N_{V_B}. \end{aligned} \quad (21)$$

Fig. 2 shows a simple example for illustration of pixel blocks with NH=8, NV= 8, and B=4, The thick lines represent
the block boundaries. The sets of pixel pairs in this example are

$$\begin{aligned} \mathcal{H}_B &= \{(y_4, y_5), (y_{12}, y_{13}), \ldots, (y_{60}, y_{61})\} \\ \mathcal{H}_B^C &= \{(y_1, y_2), (y_2, y_3), (y_3, y_4), (y_5, y_6) \\ &\quad \ldots, (y_{63}, y_{64})\} \\ \mathcal{V}_B &= \{(y_{25}, y_{33}), (y_{26}, y_{34}), \ldots, (y_{32}, y_{40})\} \\ \mathcal{V}_B^C &= \{(y_1, y_9), (y_9, y_{17}), (y_{17}, y_{25}), (y_{33}, y_{41}) \\ &\quad \ldots, (y_{56}, y_{64})\}. \end{aligned} \quad (22)$$

Then we define the mean boundary pixel squared difference (DB) and the mean non boundary pixel squared difference (DcB) for image **y** to be

$$\begin{aligned} D_B(\mathbf{y}) &= \frac{\sum_{(y_i,y_j)\in\mathcal{H}_B} (y_i - y_j)^2 + \sum_{(y_i,y_j)\in\mathcal{V}_B} (y_i - y_j)^2}{N_{H_B} + N_{V_B}} \\ D_B^C(\mathbf{y}) &= \frac{\sum_{(y_i,y_j)\in\mathcal{H}_B^C} (y_i - y_j)^2 + \sum_{(y_i,y_j)\in\mathcal{V}_B^C} (y_i - y_j)^2}{N_{H_B^C} + N_{V_B^C}}, \end{aligned} \quad (23)$$

Generally, as the quantization step size increases, (DB) will increase relative to (DcB) and blocking artifacts will become more visible. Of course, this does not establish any level of correlation between and perceptual annoyance. Also define the blocking effect factor

$$\mathrm{BEF}(\mathbf{y}) = \eta \cdot \left[D_B(\mathbf{y}) - D_B^C(\mathbf{y})\right] \quad (24)$$

Where

$$\eta = \begin{cases} \frac{\log_2 B}{\log_2(\min(N_H, N_V))}, & \text{if } D_B(\mathbf{y}) > D_B^C(\mathbf{y}) \\ 0, & \text{otherwise} \end{cases} \quad (25)$$

emphasizes the BEF as a function of block size. The assumption here is that the visibility of blocking effects increases with block size.

Of course, there can be multiple block sizes in a particular decoded image/video. For example, there can be 16 X 16 macro blocks and 4 X 4 transform blocks, both contributing to blocking effects, as in H.264 video coding

$$\mathrm{BEF}_k(\mathbf{y}) = \eta_k \cdot \left[D_{B_k}(\mathbf{y}) - D_{B_k}^C(\mathbf{y})\right] \quad (26)$$

The BEF over all block sizes is defined as

$$\mathrm{BEF}_{\mathrm{Tot}}(\mathbf{y}) = \sum_{k=1}^{K} \mathrm{BEF}_k(\mathbf{y}) \quad (27)$$

The mean-squared error including blocking effects (MSE-B)
for reference image **x** and test image **y** is then defined as the sum of the MSE **(x,y)**

$$\text{MSE-}B(\mathbf{x}, \mathbf{y}) = \mathrm{MSE}(\mathbf{x}, \mathbf{y}) + \mathrm{BEF}_{\mathrm{Tot}}(\mathbf{y}) \quad (29)$$

Finally, we propose the PSNR-B as

$$\text{PSNR-}B(\mathbf{x}, \mathbf{y}) = 10 \log_{10} \frac{255^2}{\text{MSE-}B(\mathbf{x}, \mathbf{y})} \quad (30)$$

The MSE term in measures the distortion between the reference image and the test image , while the BEF term in specifically measures the amount of blocking artifacts just using the test image . The BEF itself can be used as a no reference quality index, similar to the generalized block-edge impairment metric (GBIM) and the mean noticeable blockiness score (MNBS) [20]. These no-reference quality indices claim to be efficient for measuring the amount of blockiness, but may not be efficient for measuring image quality relative to full-reference quality assessment. On the other hand, the MSE is not specific to blocking effects, which can substantially affect subjective quality. We argue that the combination of MSE and BEF is an effective measurement for quality assessment considering both the distortions from the original image and the blocking effects in the test image. The associated quality index PSNR-B is obtained from the MSE-B by a logarithmic function, as is the PSNR from the MSE. The PSNR-B is attractive since it is specific for assessing image quality, specifically the severity of blocking artifacts.

www.ijmer.com Vol.2, Issue.4, July-Aug. 2012 pp-2615-2620 ISSN: 2249-6645

IV. MATLAB RESULTS

Now we present simulation results for de-blocking filters for H.264 video coding. The H.264 encoding and decoding simulations are performed using the H.264 reference. The in-loop de-blocking filter is a key component in H.264 video coding. If the filter is selected by an encoding parameter, in-loop filtering is performed both in encoding and in decoding. If it is not selected, in-loop filtering is not performed either in encoding or in decoding. In H.264, the quantization step size is controlled by the quantization parameter (QP) during encoding [16]. The QP can take 52 values ranging from 0 to 51, and the quantization step is doubled for each increment of six in the QP [19]. In H.264 coding, the quantization step is the same for all transform coefficients as determined by the QP. To assess the in-loop filter using the quality indices, the size of a group-of-pictures (GOP) is set as eight with one I-frame and seven P-frames. In the simulations, 16 frames are encoded and decoded. The quality indices were applied on the original (reference) and decoded images at each frame, and the quality scores were then averaged over the 16 frames

A.PSNR Analysis:

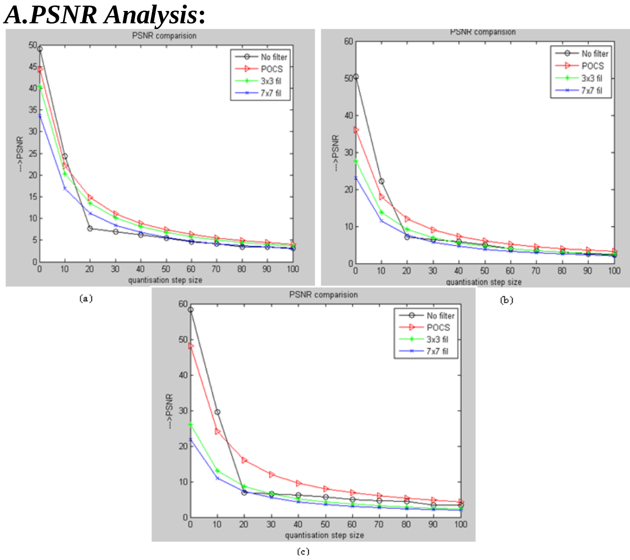

Fig. 3 PSNR comparison of filters for H.264 videos.

Fig. 3 examines the H.264 in-loop filter and low pass filters using the PSNR as an analysis tool. The 3x3 and 7x7 low pass filters do not provide improvement compared to not filtering for small to medium quantization step sizes . The low pass filters produce slight improvement compared to not filtering for on the Foreman and Mother and Daughter videos. The in-loop filter gave a slight improvement of PSNR compared to not filtering for mid-to-large quantization steps on the Foreman, Mother and Daughter, and Hall Monitor videos. The in-loop filter did not produce improvements compared to not filtering on the complex Mobile video, according to the PSNR. However, the PSNR is of dubious value when assessing perceptual quality.

B. SSIM Analysis:

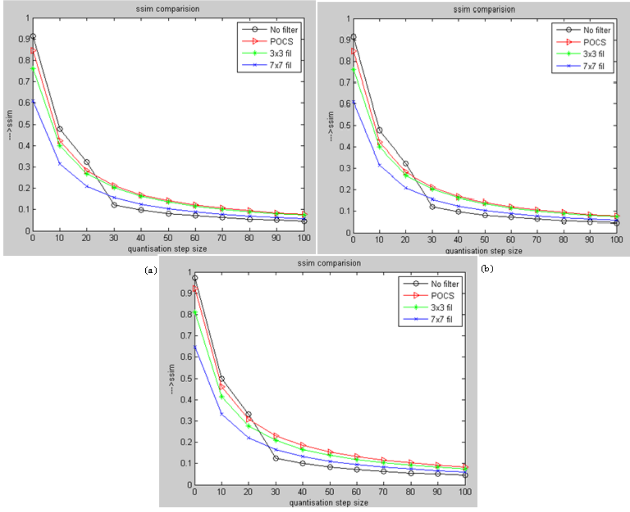

(c)

Figure 4: SSIM comparison of filters for H.264 videos

Fig. 4 studies the de-blocking methods using the SSIM index . The in-loop filter produced improvement in the SSIM values compared to not filtering for mid-to-large quantization steps on the Foreman, Mother and Daughter, and Hall Monitor videos. As the quantization step was increased, the in-loop filter systematically produced larger SSIM values. The 3x3 filter also produced improvement according to SSIM as compared to not filtering on the Foreman, Mother and Daughter, and Hall Monitor videos, when the quantization step was greater than 40. For the Mobile video, the in-loop filter produced SSIM values almost the same as those for not filtering while the low pass filters gave lower SSIM values. This is clear evidence that the in-loop filter works well, according to the perceptually relevant SSIM index.

C. PSNR-B Analysis:

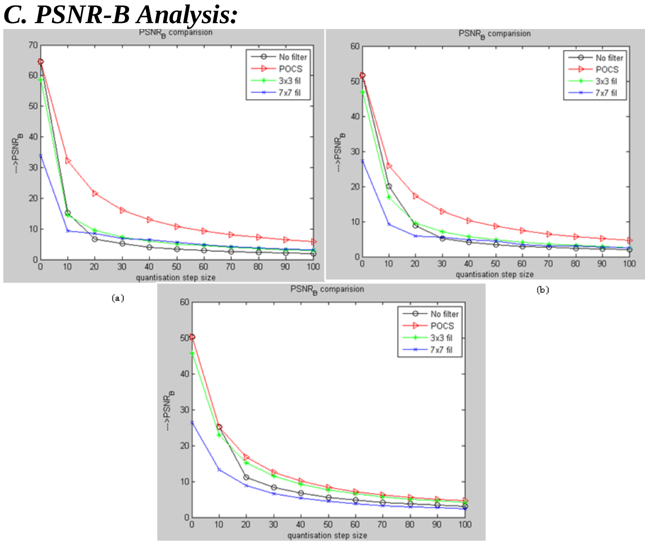

(c)

Fig. 5. PSNR-B comparison of filters for H.264 videos

Fig. 5 analyzes the in-loop filter using PSNR-B. PSNR-B produces trends similar to SSIM and visual analysis, while the PSNR shows different trends. For mid-to-large quantization steps , PSNR-B shows that the in-loop filter delivers marginal improvement as compared to not filtering, while the PSNR shows little change on the Foreman, Mother and Daughter, and Hall Monitor videos. For a large quantization step , the PSNR-B comparison in Fig. 5 shows that the 3x 3 and 7x 7 filters deliver improvements,

V. CONCLUSION

Here we proposed the block-sensitive image quality index PSNR-B for quality assessment of de-blocked images. It modifies the conventional PSNR by including an effective blocking effect factor. In simulations, we compared relevant image quality indices for de-blocked images. The simulation results show that PSNR-B results in better and good performance than PSNR for image quality assessment of these impaired images. By comparison, the blockiness-specific index GBIM effectively assesses blockiness, but has limitations for image quality assessment. PSNR-B shows similar trends with the perceptually proven index SSIM. It is attractive since it is specific for assessing image quality, specifically the severity of blocking artifacts. The PSNR-B takes values in a similar range as PSNR and is, therefore, intuitive for users of PSNR, while it results in better performance for quality assessment of de-blocked images.

References

[1] Z. Wang, A. C. Bovik, H. R. Sheikh, and E. P. Simoncelli, "Image quality assessment: From error visibility to structural similarity," *IEEE Trans. Image Process.*, vol. 13, no. 4, pp. 600–612, Apr. 2004.

[2] Z. Wang, E. P. Simoncelli, and A. C. Bovik, "Multi-scale structural similarity for image quality assessment," in *Proc. IEEE Asilomar Conf. Signal Syst. Comput.*, Nov. 2003.

[3] H. R. Sheikh and A. C. Bovik, "Image information and visual quality," *IEEE Trans. Image Process.*, vol. 15, no. 2, pp. 430–444, Feb. 2006.

[4] H. R. Sheikh and A. C. Bovik, "A statistical evaluation of recent full reference image quality assessment algorithms," *IEEE Trans. Image Process.*, vol. 15, no. 11, pp. 3441–3452, Nov. 2006.

[5] Z. Wang and A. C. Bovik, "A universal image quality index," *IEEE Signal Process. Lett.*, vol. 9, no. 3, pp. 81–84, Mar. 2002.

[6] B. Girod, "What's wrong with mean-squared error," in *Digital Images and Human Vision*, A. B. Watson, Ed. Cambridge, MA: MIT Press, 1993, pp. 207–220.

[7] Y. Yang, N. P. Galatsanos, and A. K. Katsaggelos, "Projection-based spatially adaptive reconstruction of block-transform compressed images," *IEEE Trans. Image Process.*, vol. 4, no. 7, pp. 896–908, Jul. 1995.

[8] Y. Yang, N. P. Galatsanos, and A. K. Katsaggelos, "Regularized reconstruction to reduce blocking artifacts of block discrete cosine transform compressed images," *IEEE Trans. Circuits Syst. Video Technol.*, vol. 3, no. 6, pp. 421–432, Dec. 1993.

[9] H. Paek, R.-C. Kim, and S. U. Lee, "On the POCS-based post processing technique to reduce the blocking artifacts in transform coded images," *IEEE Trans. Circuits Syst. Video Technol.*, vol. 8, no. 3, pp.358–367, Jun. 1998.

[10] S. H. Park and D. S. Kim, "Theory of projection onto narrow quantization constraint set and its applications," *IEEE Trans. Image Process.*, vol. 8, no. 10, pp. 1361–1373, Oct. 1999.

[11] A. Zakhor, "Iterative procedure for reduction of blocking effects in transform image coding," *IEEE Trans. Circuits Syst. Video Technol.*, vol. 2, no. 1, pp. 91–95, Mar. 1992.

[12] Y. Jeong, I. Kim, and H. Kang, "A practical projection-based postprocessing of block-coded images with fast convergence rate," *IEEE Trans. Circuits and Syst. Video Technol.*, vol. 10, no. 4, pp. 617–623, Jun. 2000.

[13] S. Liu and A. C. Bovik, "Efficient DCT-domain blind measurement and reduction of blocking artifacts," *IEEE Trans. Circuits Syst. Video Technol.*, vol. 12, no. 12, pp. 1139–1149, Dec. 2002.

[14] Z.Wang and A. C. Bovik, "Blind measurement of blocking artifacts in images," in *Proc. IEEE Int. Conf. Image Process.*, Vancouver, Canada, Oct. 2000, pp. 981–984.

[15] P. List, A. Joch, J. Laimena, J. Bjøntegaard, and M. Karczewicz, "Adaptive deblocking filter," *IEEE Trans. Circuits Syst. Video Technol.*, vol. 13, no. 7, pp. 614–619, Jul. 2003.

[16] *Draft ITU-T Recommendation and Final Draft International Standard of Joint Video Specification (ITU Rec. H.264—ISO/IEC 14496-10 AVC)*, , 2003, Doc.JVT-G050.

[17] T. Wiegand, G. Sullivan, J. Bjøntegaard, and G. A. Luthra, "Overview of the H.264/AVC video coding standard," *IEEE Trans. Circuits Syst. Video Technol.*, vol. 13, no. 7, pp. 560–576, Jul. 2003.

[18] H.264/AVC Software Co-ordination [Online]. Available: http:// iphome.hhi.de/suehring/tml/index.htm

[19] I. E. G. Richardson, *H.264 and MPEG-4 Video Compression*. Hoboken, NJ: Wiley, 2003.

[20] H. R. Wu and M. Yuen, "A generalized block-edge impairment metric for video coding," *IEEE Signal Process. Lett.*, vol. 4, no. 11, pp. 317–320, Nov. 1997.

[21] G. Zhai, W. Zhang, X. Yang, W. Lin, and Y. Xu, "No-reference noticeable blockiness estimation in images," *Signal Process. Image Commun.*, vol. 23, pp. 417–432, 2008.